# A physical gel made from hyperbranched polymer gelator

Yongwen Zhang, Wei Huang*, Yongfeng Zhou and Deyuan Yan*



## S1 Experimental Section

### S1.1 Materials

*N,N′*-methylene bisacrylamide (MBA) and 1-(2-aminoethyl)piperazine (AEPZ) were purchased from Acros and used as received. All the solvents including DMF, DMAC, NMP and pyridine were analytic reagents and purified before use.

### S1.2 Polymerization

**Synthesis of HPMAs.** The typical polymerization was as follows (e.g., HPMA-1): 3.083 g MBA (20 mmol) was added into a solution of 2.584 g AEPZ (20 mmol) in 30 mL deionized water. The polymerization was performed at 30 $^{o}$C for 60 h under vigorous stirring. The resulting solution was precipitated in acetone to produce viscous solid. Then it was purified by a silicon gel column to remove the possible slight crosslinking materials. HPMA-1 was obtained by drying at 50 $^{o}$C under vacuum for 48 h. Other samples in Table 1 were prepared by the same procedure at the different feed molar ratio of MBA to AEPZ.

**Synthesis of HPMA Hydrochlorate.** Typically, 3.083 g MBA (20 mmol) was added into a solution of 2.584 g AEPZ (20 mmol) in 30 mL deionized water. The polymerization was performed at 30 $^{o}$C for 60 h under vigorous stirring. Then 10 mL of hydrochloric acid (8M) was added into the solution and stirred for another 5 h at 30 $^{o}$C. The resulting solution was condensed by rotary evaporation and then purified in the same way as HPMAs.

**Synthesis of HPMA-vinyl.** HPMA-vinyl was prepared as described previously.[1] 2.584 g AEPZ (20 mmol) was added into a solution of 6.164 g MBA (40 mmol) in 60 mL deionized water/$CH_3OH$ (1/2 in volume ratio). The polymerization was carried out at 50 $^{o}$C for one week under vigorous stirring. The resulting viscous solution was concentrated by rotary evaporation and then precipitated

in 300 mL acetone. The product was purified by reprecipitating three times. HPMA-vinyl was obtained by drying at 50 $^{o}$C under vacuum for 48 h.

**S1.3 Characterization**

**Nuclear Magnetic Resonance (NMR).** $^{1}$H NMR and $^{13}$C NMR were tested on a MERCURY plus-400 spectrometer (Varian, Inc., USA) at 20 $^{o}$C in DMSO-$d_6$. Quantitative $^{13}$C NMR spectra were measured by the method of inverse-gated broadband decoupling. $^{1}$H-$^{1}$H COSY and $^{13}$C-$^{1}$H HSQC spectra were recorded using the standard pulse sequence provided by Varian.

**Gel Permeation Chromatography (GPC).** The molecular weight and molecular weight distribution were determined by gel permeation chromatography (GPC). It was carried out on a Perkin-Elmer Series 200 system at 70 °C (100 mL injection column, PL gel 10 μm 300 × 7.5 mm mixed-B columns, polystyrene calibration). DMF was used as the eluent and the flow rate was 1.0 mL min$^{-1}$.

**Fourier Transform Infrared Measurements (FTIR).** FTIR spectra were recorded on an EQUINOX 55 spectrometer using KBr window and all the measurements were performed at ambient temperature (ca. 25 $^{o}$C).

**Differential Scanning Calorimetry (DSC).** The glass transition temperatures ($T_g$) of the obtained hyperbranched polymers were determined using a Perkin-Elmer Pyris 1 differential scanning calorimeter under a dry nitrogen atmosphere with a heating rate of 10 $^{o}$C min$^{-1}$ from 0 to 100 $^{o}$C and the results were obtained in the second scan.

**Thermo Gravimetric Analysis (TGA).** TGA was performed on a PERKIN-ELMER with a heating rate of 20 $^{o}$C min$^{-1}$ under a nitrogen atmosphere.

**X-Ray Diffraction (XRD).** Glass plates with dry gels were fixed on a sample holder and subjected to XRD analysis a room temperature on a D/MAX-2200/PC diffractometer. XRD patterns were recorded at a scanning rate of 4$^{o}$ min$^{-1}$ in the 2θ range of 25 to 80 with Cu Kα radiation (λ = 1.54178 Å).

**Cryo-TEM Imaging**. Ultramicrocuts of gels (ca. 80 nm thick) were obtained under -80 $^{o}$C by an ultramicrotome. The ultramicrocuts were then moved onto the 230 mesh polymer-coated copper grids under a low temperature. The frozen samples were imaged on a JEM-1200EX microscope under liquid nitrogen temperature, operating at 60 kV using a Gatan low temperature sample stage. The objective lens was underfocused to enhance the phase shift between the vitrified solvent and the microstructure of the gelator. By this attempt, the contrast in the image was achieved.

**Rheological Measurements.** Viscoelastic measurements of the gels were conducted on a rheometer ARES-RFS (TA Co., USA), equipped with a Peltier device for temperature control (within 0.1 $^{o}$C). A ConiCylinder geometry (outer diameter = 17 mm; inter diameter =14 mm; gap = 2

mm) was employed. During all rheological experiments, a solvent trap with methyl silicone oil was used to avoid evaporation and moisture absorption.

## S2 Discussion on Polymerization

$^1$H NMR spectra were used to trace the polymerization process as shown in Fig. S1. The vinyl signals at ca. 5.6 and 6.2 ppm decreased gradually with the polymerization going on. The conversion of double bonds in MBA could be calculated by $^1$H NMR based on Equation (1).

$$C_{\text{double bonds}}\% = (1 - I_{5.56\text{-}6.30}/3I_{4.27\text{-}4.56})\times 100\% \quad (1)$$

where $I_{5.56\text{-}6.30}$ and $I_{4.27\text{-}4.56}$ were the integral intensities of the signals at ca. 5.56-6.30 and 4.27-4.56 ppm, which were attributed to the protons attached to the carbons in vinyl groups and the methylene in -CONHCH$_2$CONH- units, respectively. After reacting for 5 min, the conversion of the double bonds in MBA reached ca. 78%, and 92% for 1 h. This means that the addition reaction was very fast at the initial period of the polymerization. After 10 h the signals of vinyl groups disappeared completely, indicating the retro-Michael addition could be negligible.

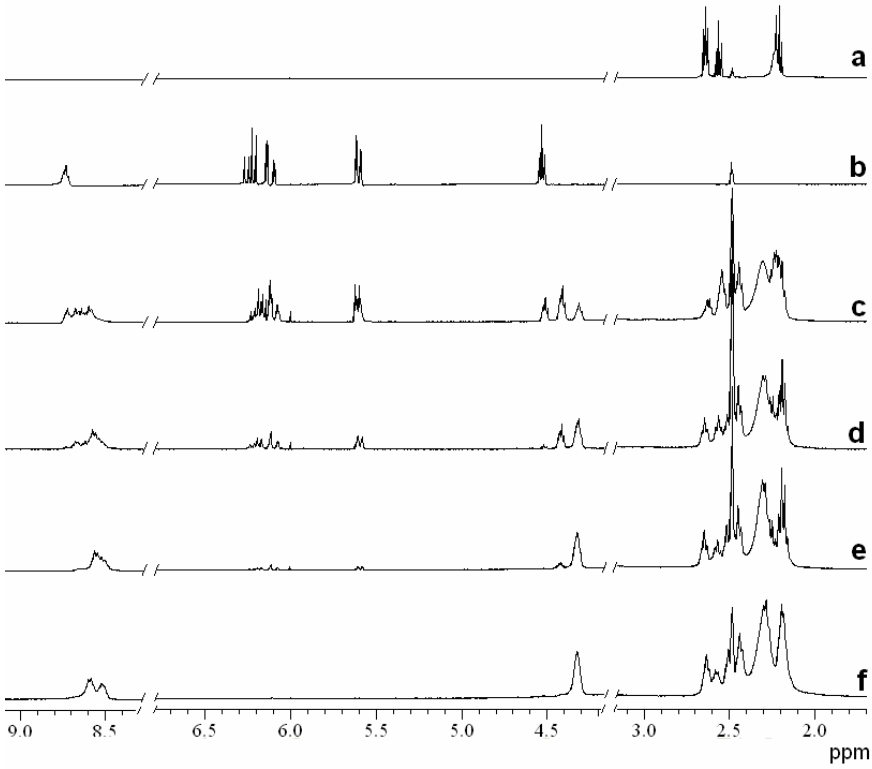


**Fig. S1.** $^1$H NMR spectra of monomers (a) AEPZ; (b) MBA; and the $^1$H NMR spectra recorded for the polymerization of MBA with equal molar AEPZ in $H_2O$ at 30 $^o$C: (c) 5 min, (d) 1 h, (e) 3 h, and (f) 10 h.

In order to identify the reaction mechanism, the polymerization was monitored by $^{13}$C NMR spectrum in situ. The results are shown in Fig. S2. The ascription of the signals in the $^{13}$C NMR was

based on the 2D NMR in the next section. At the beginning of the reaction, Fig. S2a shows that most of highly reactive $2^o$ amines (original) reacted with MBA to form Intermediate I as indicated by the signals such as $b_2$ at 59.5 ppm. Meanwhile, the appearance of the relatively weak signals such as $d_3$ at 44.6 ppm indicated that only a little amount of $2^o$ amines (derived) were formed. In general, the reaction predominantly results in the $AB_2$ intermediates at the beginning. This is reasonable due to the lower reactivity of $1^o$ amines comparing with that of $2^o$ amines (original). Fig. S2b shows that the signals of AEPZ (such as $b_1$ at 60.2 ppm) disappeared and the amount of $2^o$ amines (derived) increased when the polymerization was performed for ca. 0.5 h. As the polymerization going on, $2^o$ amines (derived) further participated in the polymerization to form tertiary amines (e.g., the signals of $e_4$, $f_4$, $g_4$ and $h_4$ at ca. 54.5, 53.16, 49.06 and 32.5 ppm respectively in Fig. S2c).

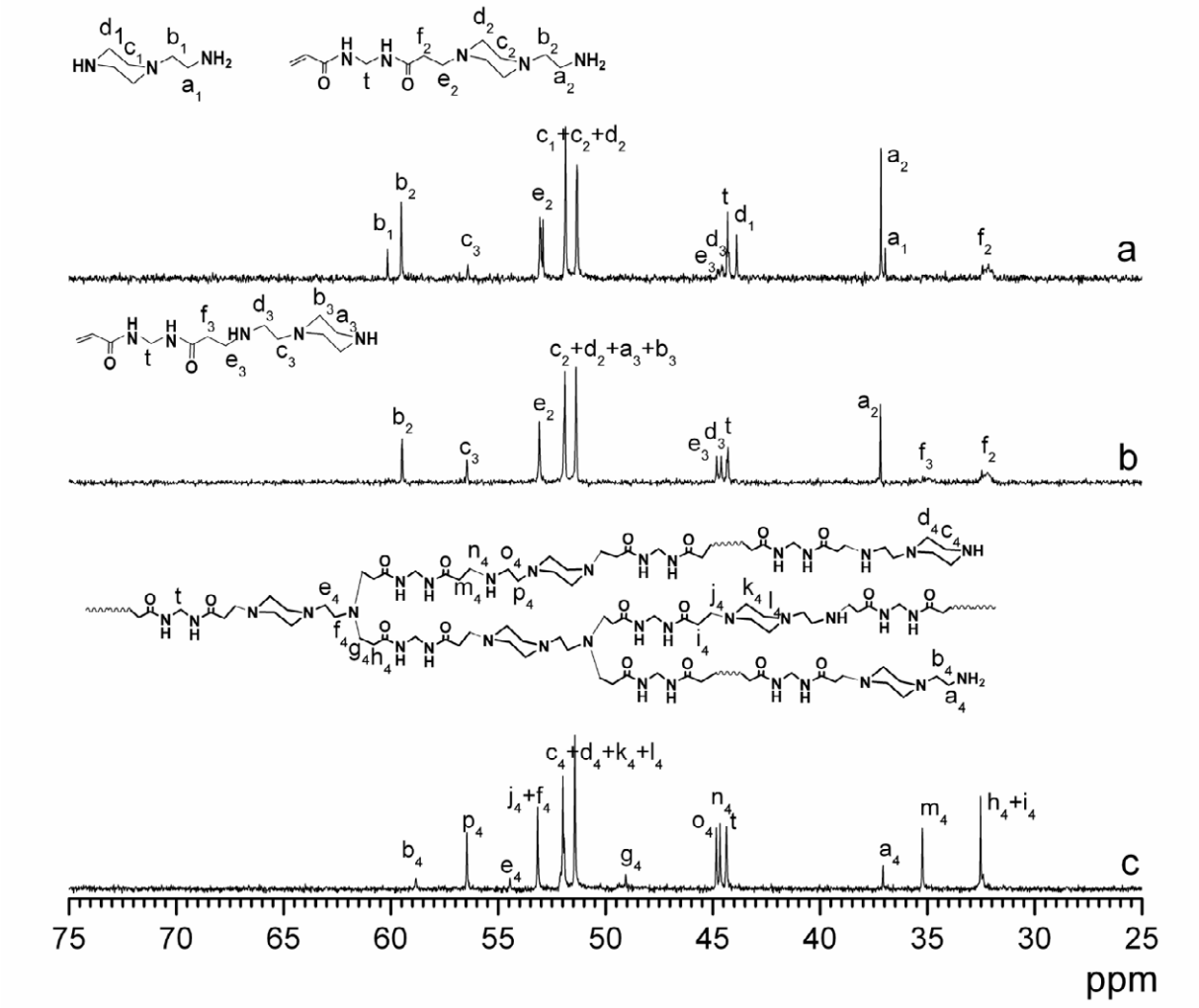


**Fig. S2.** $^{13}C$ spectra recorded in situ for the polymerization of HPMA-1 in $D_2O$ at 30 $^oC$: (a) 5 min; (b) 0.5 h; (c) 10 h.

## S3 Determination of the Degree of Branching

The degree of branching (DB) is the most important molecular parameter for hyperbranched polymers. Generally, hyperbranched polymers consist of dendritic, linear and terminal units. There are five possible structural units generated from the polymerization of MBA and AEPZ as listed in Chart S1.

**Chart S1.** Structural units in HPMA generated from the polymerization of MBA and AEPZ

**Linear Unit (L)**

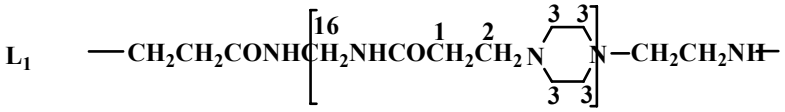


**Dendritic Unit (D)**

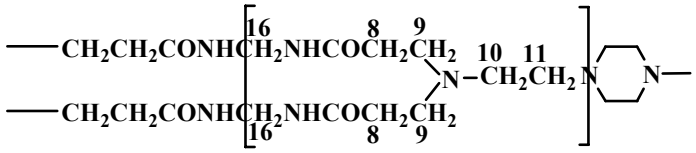


**Terminal Unit (T)**

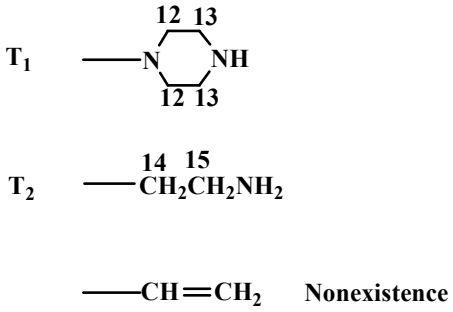


In Chart S1, each methylene in various structural units is labeled. Identification of these structural units in the spectra is assisted by the NMR spectra of the monomers and 2D NMR of HPMA. Combining the $^{13}C$-$^{1}H$ HSQC spectra in Fig. S3a with the $^{1}H$-$^{1}H$ COSY spectra in Fig. S3b, the detailed assignment of the 16 sorts of methylenes in HPMA is shown in Fig. S4. Then the DB can be calculated according to Formula (2):[2]

$$DB = (D+T)/(D+T+L) = (D+T_1+T_2)/(D+T_1+T_2+L_1+L_2) \quad (2)$$

Where, D, $T_1$, $T_2$, $L_1$ and $L_2$ represent the fractions of dendritic units (D), terminal units ($T_1$, $T_2$), and linear units ($L_1$, $L_2$), respectively. Table 1 shows that the DB values of the hyperbranched gelators range from 0.38 to 0.43.

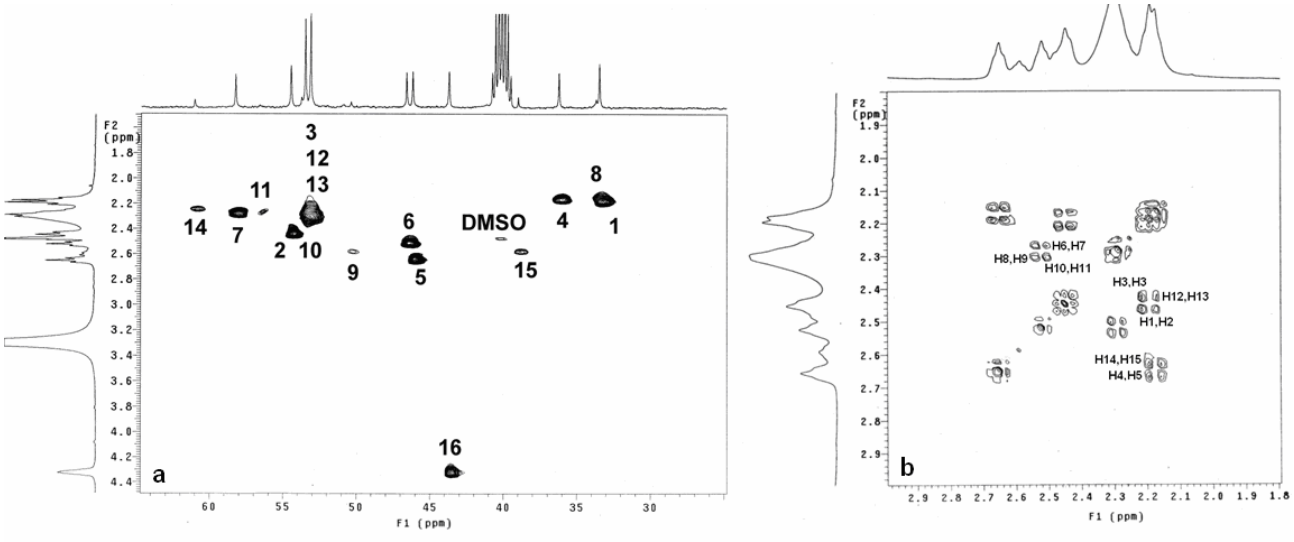


**Fig. S3.** (a) $^{13}C$-$^{1}H$ HSQC spectrum of HPMA-1 in DMSO-$d_6$; (b) $^{1}H$-$^{1}H$ COSY spectrum of HPMA-1 in DMSO-$d_6$.

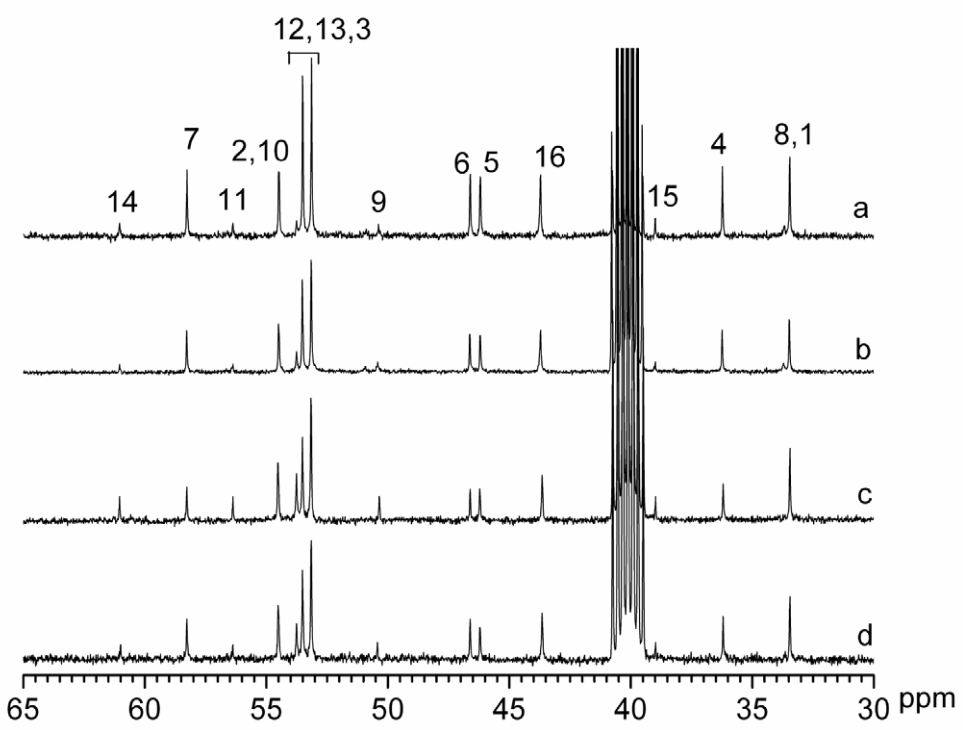


**Fig. S4.** Enlarged quantitative $^{13}C$ NMR spectra of (a) HPMA-1, (b) HPMA-2, (c) HPMA-3 and (d) HPMA-4 in DMSO-$d_6$.

**S4 Critical Gelation Concentration (CGC) Measurements.**

All samples with different concentrations were prepared by the same heating/cooling cycle in the gel preparation and the resulting solutions were kept in sealed bottles at ambient temperature for one week. The determination of gelation was made by tilting the bottles for 5 mins. If there was no flow, the sample was considered being gelled.

**Table S1.** CGC of HPMAs in Different Solvents (mg $mL^{-1}$)[a]

| | $CGC_{in\ DMF}$ | $CGC_{in\ DMAC}$ | $CGC_{in\ pyridine}$ | $CGC_{in\ DMSO}$ | $CGC_{in\ NMP}$ |
|---|---|---|---|---|---|
| HPMA-1 | 2.5 | 8 | 22 | 76 | 88 |
| HPMA-2 | 4.5 | 10 | 30 | 95 | - |
| HPMA-3 | 7.5 | 19 | 46 | - | - |
| HPMA-4 | 14 | 36 | 96 | - | - |

[a] CGC measurements were performed in the concentration range from 0 to 100 mg $mL^{-1}$;

- suggests that no gelation was observed in this concentration range.

## S5 Rheological Behavior of the Physiccal Gel

HPMA-1 gels in DMF were chosen to investigate the rheological properties. Fig. S5a was the frequency spectra obtained from the 0.5% HPMA-1 gel in DMF at 25 ℃. It was clear that *G'* was virtually independent on $\omega$ over two orders of magnitude at 1% strain, which was consistent with the dynamic mechanical behavior of physical gels. Another noteworthy feature of Fig. 5a was that *G'* exceeded *G''* over the entire range of examined $\omega$ by ca. an order of magnitude. This characteristic likewise was indicative of a physical gel. In order to discern whether the preceding frequency spectra reside within the linear viscoelastic regime, dynamic strain sweeps were likewise conducted at 25 ℃. As shown in Fig. S5b, *G'* was consistently observed to remain invariant over a finite range of strain ($\gamma^0$). This range was the corresponding linear viscoelastic range.[3]

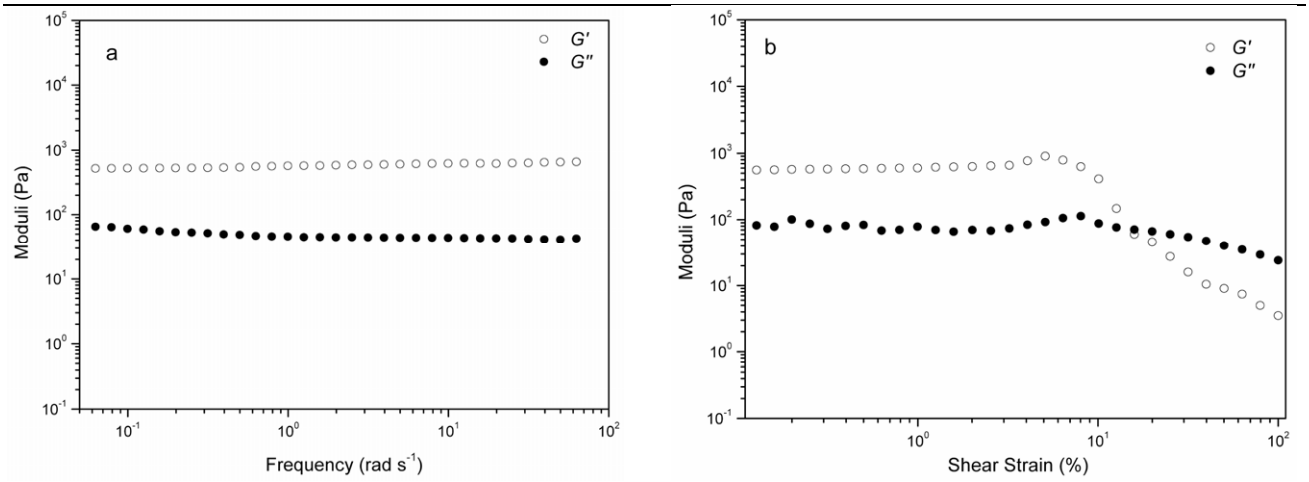


**Fig. S5.** (a) Frequency dependence of *G'* and *G''* on frequency for HPMA-1 gel in DMF at 5 mg $mL^{-1}$ using $\gamma^0$ = 0.01 and *T* =25 °C. (b) Strain dependence of *G'* and *G''* for HPMA-1 gel in DMF at 5 mg $mL^{-1}$ using $\omega$ = 1 rad $s^{-1}$ and *T* =25 °C.

Then the continuous thermal tests were performed in the linear viscoelastic range at $\omega$ = 1 rad $s^{-1}$ and $\gamma^0$ = 1.0 %. As shown in Fig. S6, under the same temperature, *G'* of the gel increased dramatically by several orders of magnitude when the concentration of HMPM-1 changed from 5 to 50 mg $mL^{-1}$. The reason is that the intermolecular interaction became stronger and the intensity of the network greatly increased with increasing the concentration of the gelator. On the other hand, both *G'* decreased sharply with increasing temperature and finally met with *G''* at a very low constant. On heating, hydrogen bonds among the macromolecules were destroyed and the gelation ability was weakened. At last the gel network was broken down to form the clear solution. The gel region was determined based on a sol-gel transition occurring at a temperature where *G'* = *G''*,[4] as shown by the arrows in Fig. S6. This gel region was in good agreement with the visualization of the gelation by the tube inversion method.

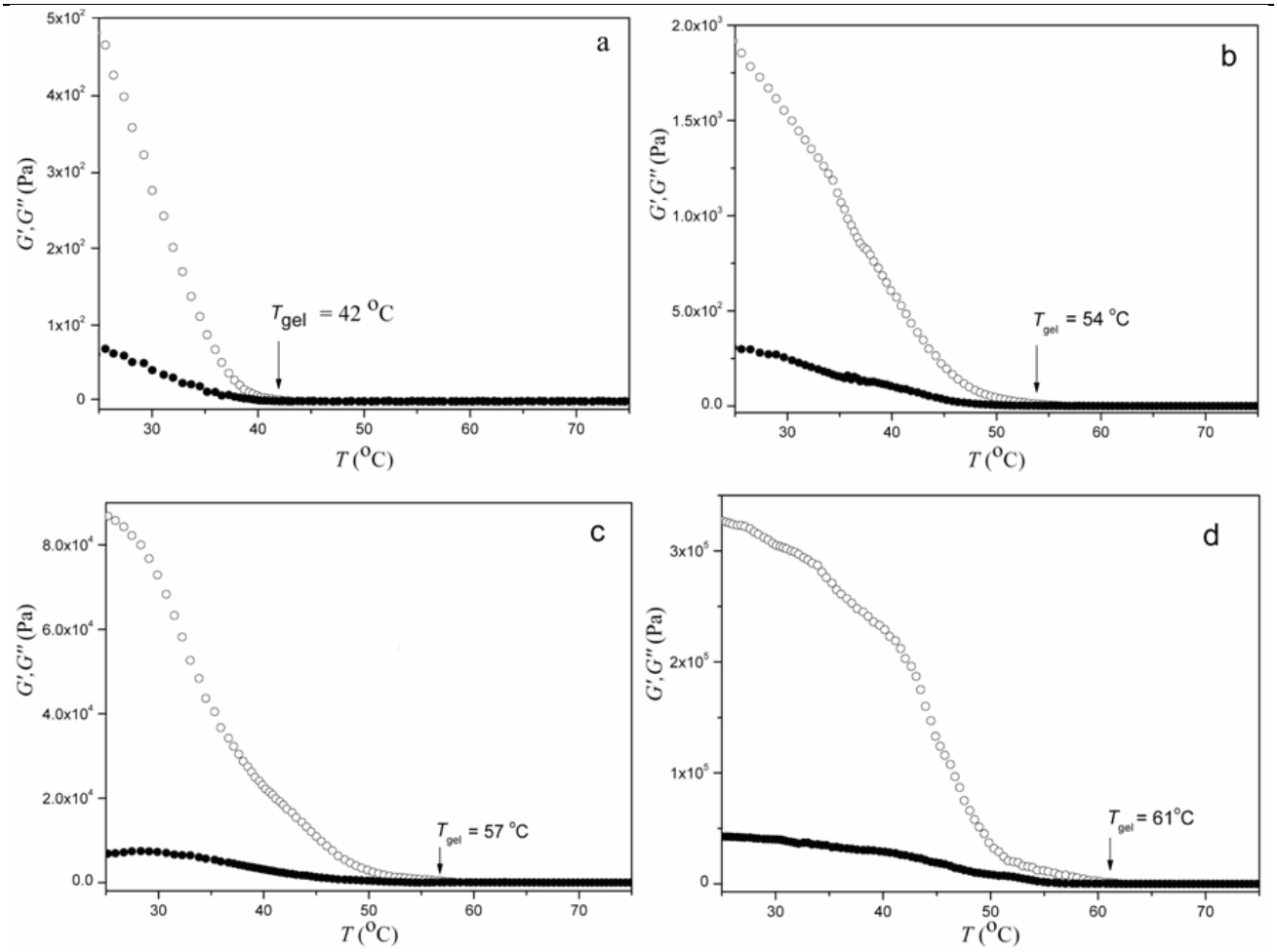


**Fig. S6.** Rheological measurements (elastic moduli *G'*(o) and viscous modulus *G''* (●)) for thermoresersible gels with different concentrations of HPMA-1 in DMF: (a) 5 mg $mL^{-1}$; (b) 10 mg $mL^{-1}$; (c) 25 mg $mL^{-1}$; (d) 50 mg $mL^{-1}$.

## S6 Others

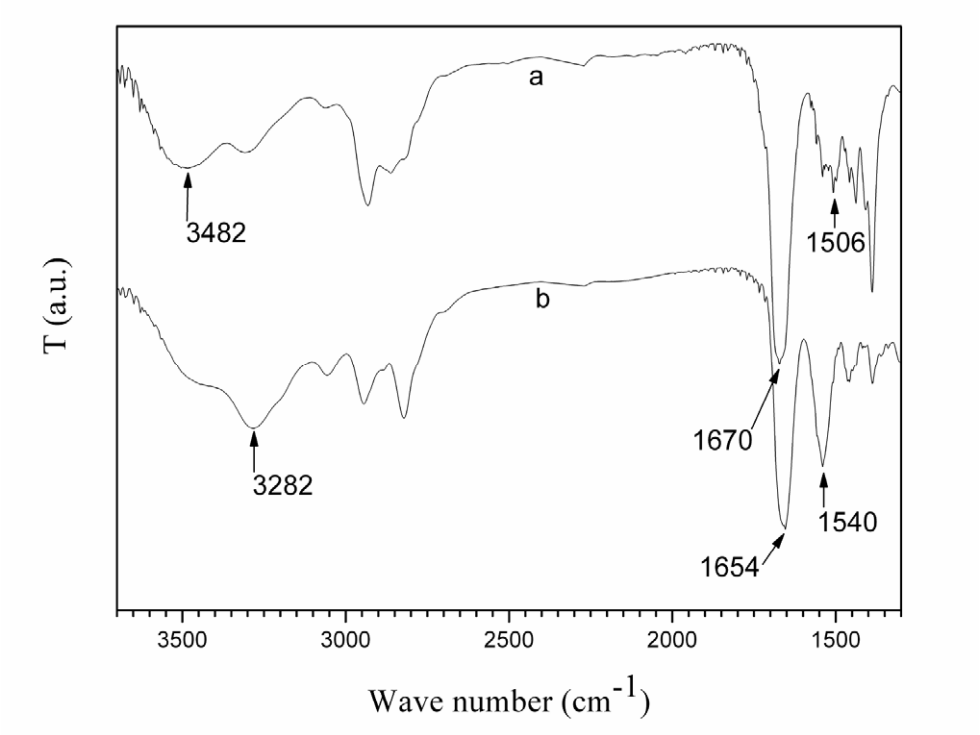


**Fig. S7.** FTIR spectra of HPMA in DMF at 25 mg $mL^{-1}$. (a) solution; (b) gel.

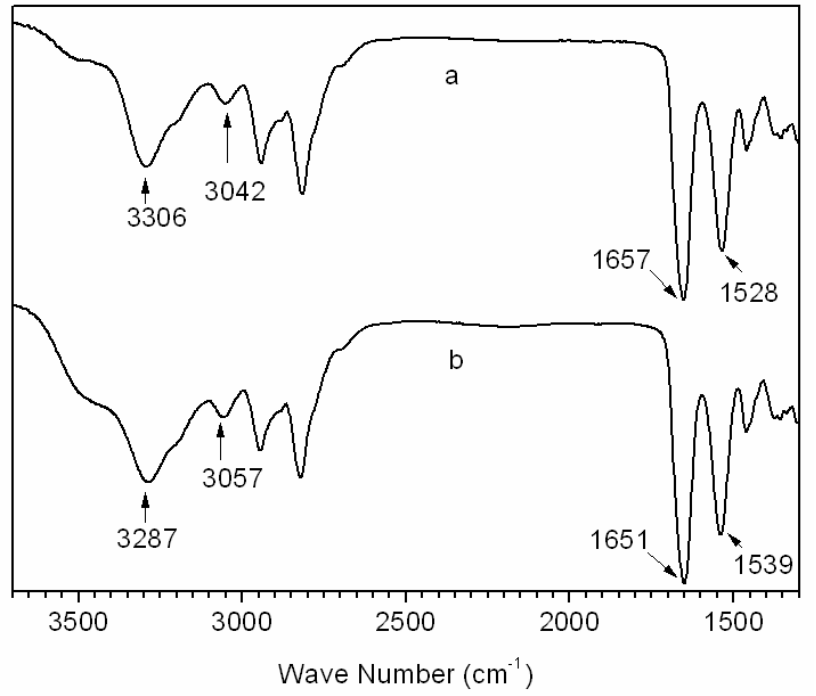


**Fig. S8.** FTIR spectra of HPMA in DMF at 10 mg $mL^{-1}$ (a) after adding 1 wt% LiBr (being the solution), and (b) before adding LiBr (being the gel).

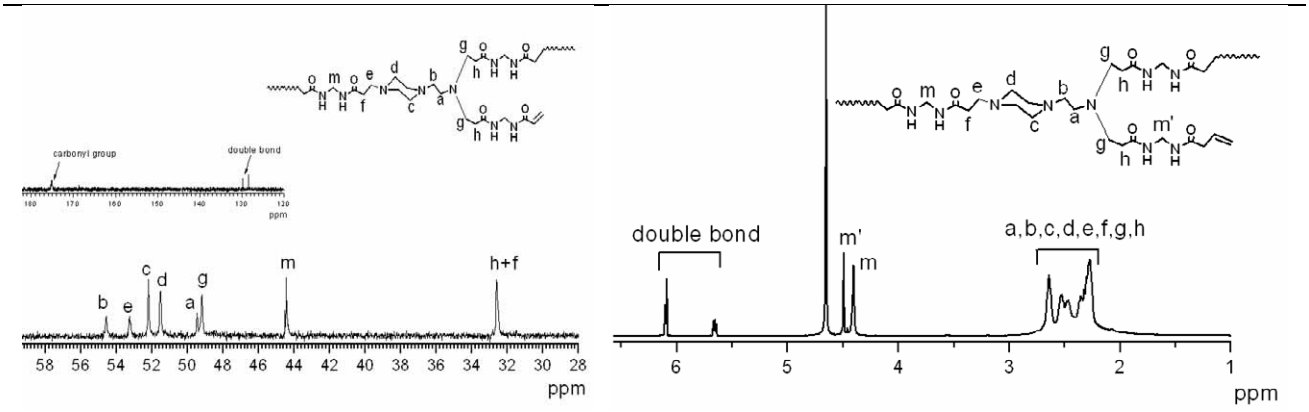


**Fig. S9.** $^{13}C$ and $^{1}H$ NMR spectra of HPMA-vinyl in $D_2O$.

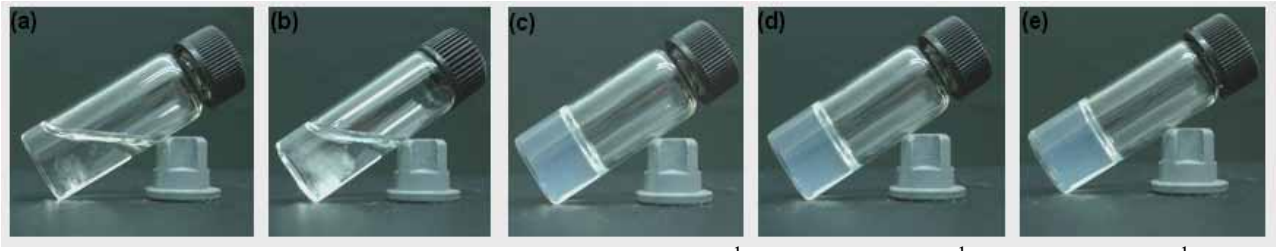


**Fig. S10.** Pictures of HPMA-1 in DMF at (a) 1.0 mg $mL^{-1}$; (b) 2.0 mg $mL^{-1}$; (c) 2.5 mg $mL^{-1}$; (d) 20 mg $mL^{-1}$; (e) 40 mg $mL^{-1}$. The flocs are visible in the flasks below the CGC (see a and b). The immobile gels are formed at or above the CGC (see c, d and e).

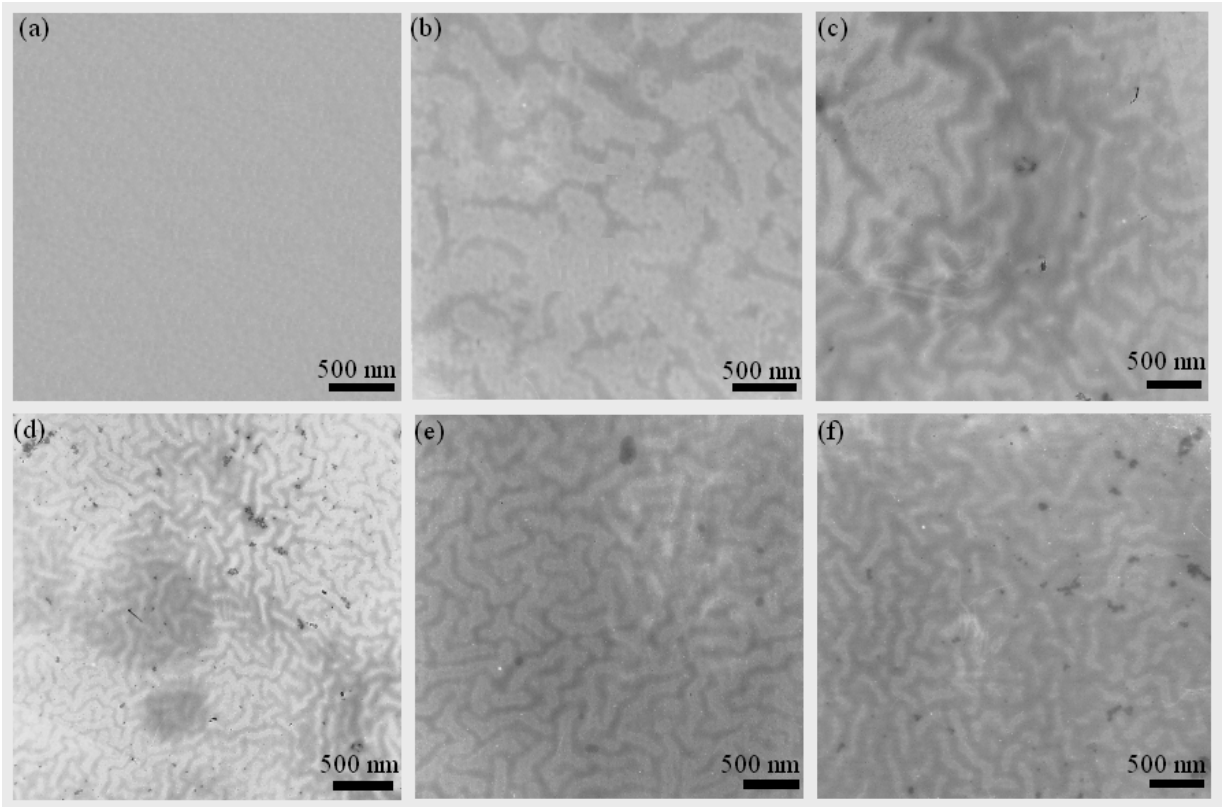

**Fig. S11.** Cryo-TEM images of HPMA-1 in DMF in upturned flasks at (a) 0 mg $mL^{-1}$ (the blank sample); (b) 1.0 mg $mL^{-1}$; (c) 2.0 mg $mL^{-1}$; (d) 2.5 mg $mL^{-1}$; (e) 20 mg $mL^{-1}$; (f) 40 mg $mL^{-1}$.

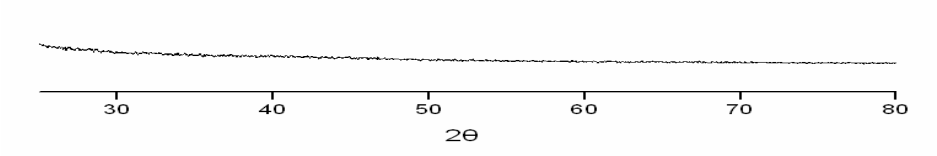


**Fig. S12.** XRD pattern of the xerogel made from HPMA-1 gel (10 mg $mL^{-1}$ in DMF).

**Supporting Notes and References**

(1) Decheng Wu, Ye Liu, Ling Chen, Chaobin He, Tai Shung Chung, Suat Hong Goh, *Macromolecules* **2005**, 38, 5519.

(2) (a) Hawker C. J., Lee R., Fréchét J. M. J., *J. Am. Chem. Soc.* **1991**, *113*, 4583; (b) Yan D. Y., Muller A. H. E., Matyjaszewski K., *Macromolecules* **1997**, *30*, 7024.

(3) (a) Frédéric Bossard, Vasiliki Sfika, Constantins Tsitsilianis, *Macromolecules* **2004**, *37*, 3899; (b) Frédéric Bossard, Constantinos Tsitsilianis, Spyros N. Yannopoulos. *Macromolecules* **2005**, *38*, 2883.

(4) (a) Emmanuel Stiakakis, Dimitris Vlassopoulos, Jacques Roovers. *Langmuir* **2003**, *19*, 6645; (b) Shinji Sugihara, Shokyoku Kanaoka, Sadahito Aoshima, *Macromolecules* **2005**, *38*, 1919; (c) Abdeslam El Ghzaoui, Fabienne Gauffre, Anne-Marie Caminade, Jean-Pierre Majoral, Hélène Lannibois-Drean, *Langmuir* **2004**, *20*, 9348.